

## Expanding Cavitand Chemistry: The Preparation and Characterization of $[n]$ Cavitands with $n \geq 4$

Christoph Naumann,<sup>[a]</sup> Esteban Román,<sup>[b]</sup> Carlos Peinador,<sup>[b, c]</sup> Tong Ren,<sup>[b]</sup>  
Brian O. Patrick,<sup>[a]</sup> Angel E. Kaifer,<sup>\*[b]</sup> and John C. Sherman<sup>\*[a]</sup>

**Abstract:** The preparation of cavitands composed of 4, 5, 6, and 7 aromatic subunits ( $[n]$ cavitands,  $n = 4-7$ ) is described. The simple, two-step synthetic procedure utilized readily available starting materials (2-methylresorcinol and diethoxymethane). The two cavitand products having 4 and 5 aromatic subunits exhibited highly symmetric *cone* conformations, while the larger cavitands ( $n = 6$  and 7) adopt conforma-

tions of lower symmetry. <sup>1</sup>H NMR spectroscopic studies of [6]cavitand and [7]cavitand revealed that these hosts undergo exchange between equivalent conformations at room temperature. The departure of these two cavitands

from cone conformations is related to steric crowding on their Ar-O-CH<sub>2</sub>-O-Ar bridges and is predicted by simple molecular mechanics calculations (MM2 force field). X-ray diffraction studies on single crystals of the [4]cavitand, [5]cavitand, and [6]cavitand hosts afforded additional experimental support for these conclusions.

**Keywords:** cavitands · chemical exchange · host-guest chemistry · supramolecular chemistry

### Introduction

According to Cram's definition,<sup>[1]</sup> "Cavitands are synthetic organic compounds with enforced cavities large enough to complex complementary organic compounds or ions." In order to develop compounds that would fit this definition, Cram and co-workers prepared a large number of cavitands starting from the acid-catalyzed condensation of resorcinol and 2-substituted resorcinols with a series of aldehydes.<sup>[2]</sup> This condensation reaction yields the cyclic tetrameric octol (resorcinarene) with  $C_{4v}$  symmetry in which the aldehyde R groups (the so-called *feet*) are all in axial positions.<sup>[3, 4]</sup>

Hydrogen bonding among the hydroxyl groups fosters the organization of the octols into flexible bowl-shaped structures. This conformation can be fixed by replacing the network of hydrogen bonds with covalent bonds, in a reaction that involves four ring closures.<sup>[5]</sup> The resulting cavitands have been used extensively by the Cram group and others not only as receptors, but also as components for the preparation of more elaborate hosts, such as carcerands and hemicarcerands.<sup>[6]</sup>

Usually, the most popular hosts in supramolecular chemistry are available in an assortment of sizes. For instance, the calix $[n]$ arenes have been prepared with  $n$  values as large as 20<sup>[7]</sup> and the unmodified cyclodextrins<sup>[8]</sup> (CDs) are commercially available with  $n = 6$  ( $\alpha$ -CD), 7 ( $\beta$ -CD), and 8 ( $\gamma$ -CD). In sharp contrast to this, the chemistry of cavitands has only made use of the cyclic tetramers ( $n = 4$ ) produced in the condensation of resorcinols with aldehydes. Thermodynamically, the  $C_{4v}$  tetramers are the most stable products of these reactions, but it has been known for years that other stereoisomers and oligomeric materials are also formed.<sup>[9]</sup> Recently Konishi et al. demonstrated that resorcin[5]arene and resorcin[6]arene cyclocondensation products can be isolated from the reaction of 2-alkylresorcinols with formaldehyde.<sup>[10, 11]</sup> These higher resorcinarenes are favored kinetically and can be obtained using shorter reaction times. As the reaction is allowed to proceed for longer times, the yields of resorcin[5]arene and resorcin[6]arene decrease and, eventually, only resorcin[4]arene can be isolated. Inspired by these findings we have started a research program targeting the preparation of

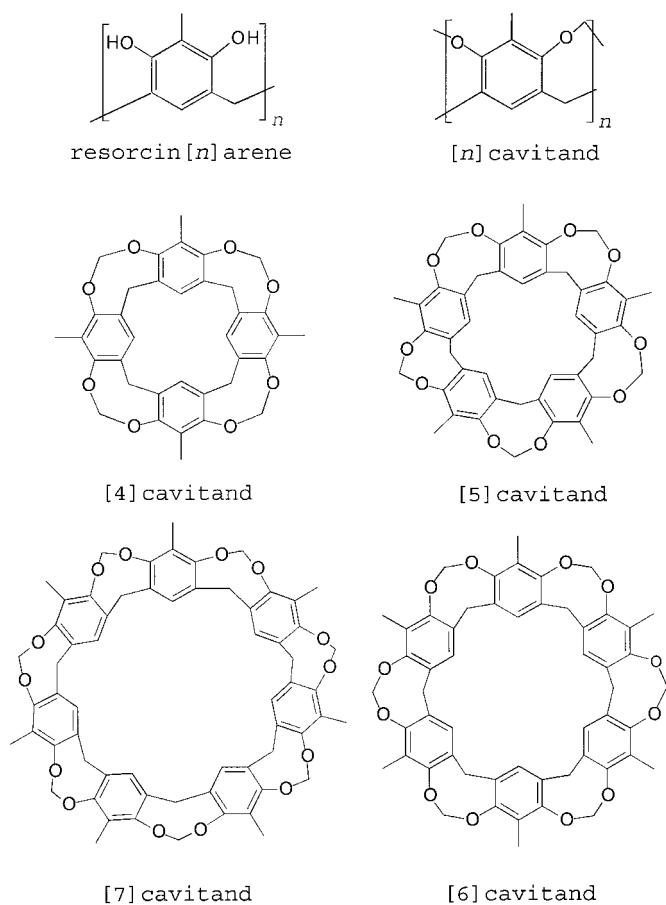
[a] Prof. Dr. J. C. Sherman, C. Naumann, Dr. B. O. Patrick  
Department of Chemistry, University of British Columbia  
2036 Main Mall, Vancouver, BC, V6T 1Z1 (Canada)  
E-mail: sherman@chem.ubc.ca

[b] Prof. Dr. A. E. Kaifer, E. Román, Dr. C. Peinador, T. Ren  
Center for Supramolecular Science and Department of Chemistry  
University of Miami, Coral Gables, FL 33124-0431 (USA)  
E-mail: akaifer@miami.edu

[c] Dr. C. Peinador  
Permanent address: Departamento de Química  
Fundamental e Industrial  
Universidad de La Coruña, Campus de La Zapateira  
15071 La Coruña (Spain)

Supporting information for this article is available on the WWW under <http://www.wiley-vch.de/home/chemistry/> or from the corresponding authors: 1. Analysis of EXSY spectra. 2. <sup>1</sup>H NMR spectrum of [7]cavitand in [D<sub>7</sub>]DMF at 400 MHz at  $-15^{\circ}\text{C}$ . Summary of all NOEs observed for [7]cavitand in [D<sub>7</sub>]DMF at  $-40^{\circ}\text{C}$ .

larger cavitands and related hosts. In this paper,<sup>[12]</sup> we report the synthesis and characterization of the first series of  $[n]$ cavitands, where  $n=4, 5, 6,$  and  $7$ .<sup>[13]</sup>



## Results and Discussion

**Synthesis:** After 48 h in ethanol solution, the HCl-catalyzed reaction of 2-methylresorcinol with formaldehyde produced the corresponding resorcin[4]arene in 73% yield. The resulting [4]cavitand was subsequently obtained in 83% using our previously reported bridging procedure.<sup>[14]</sup> In agreement with the results of Konishi and co-workers,<sup>[10, 11]</sup> the acid-catalyzed condensation of 2-methylresorcinol with formaldehyde leads to a mixture of resorcinarenes when stopped at much shorter reaction times (e.g. 30 min). The resulting mixture was treated with  $\text{CH}_2\text{BrCl}$  to produce the corresponding mixture of cavitands. FAB and Maldi-Tof (using *p*-nitroaniline as matrix) mass spectrometric data of this mixture quickly revealed the presence of four  $[n]$ cavitands, with  $n=4, 5, 6,$  and  $7$ . [5]Cavitand and [6]cavitand were separated from [4]cavitand and [7]cavitand by their low solubility in ethyl acetate. Even though the yields obtained for the cavitands are low ([4]cavitand, 3.6%; [5]cavitand, 3.6%; [6]cavitand, 13.9%; and [7]cavitand, 1.1%), they can be produced on multi-gram scales. Moreover, it is far easier to purify the cavitand mixture than to isolate the different resorcinarene products and bridge them separately.

**Characterization of [4]cavitand and [5]cavitand:** [4]Cavitand is the first reported cavitand without “feet”, that is, obtained from condensation with formaldehyde. The absence of substituents in its lower rim does not introduce any significant structural changes as compared to other tetrameric cavitands. Therefore, this cavitand exhibits a  $^1\text{H}$  NMR spectrum (see Figure 1) that suggests a highly symmetric ( $C_{4v}$ ) cone con-

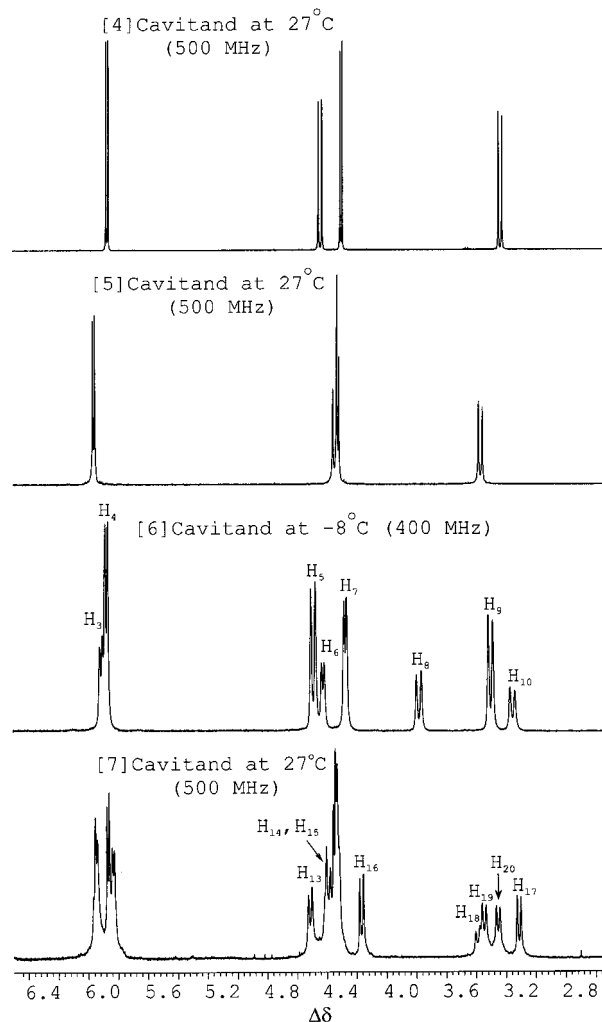


Figure 1. Parts of the  $^1\text{H}$  NMR spectra of  $[n]$ cavitands ( $n=4-7$ ). The aromatic protons and the methyl protons are not shown. All spectra were recorded in  $\text{CDCl}_3$ . See Figure 5a for labels of the [6]cavitand. Labels for the [7]cavitand are given in Figure 5b and a complete assignment of all protons can be found in the Supporting Information.

formation (singlet for the aromatic protons, doublets for the outside and inside groups of protons in the  $\text{OCH}_2\text{O}$  bridges, as well as for the  $\text{ArCH}_2\text{Ar}$  bridges, and singlet for the benzylic methyl protons). This conformation was clearly verified by the results of X-ray diffraction analysis on single crystals of this compound (Figure 2).

The  $^1\text{H}$  NMR spectrum of the [5]cavitand shows a singlet at  $\delta=7.18$  for the aromatic protons and another singlet at  $\delta=2.06$  for the methyl protons. The four sets of bridge protons also appear in the expected four-doublet pattern (Figure 1). The  $^{13}\text{C}$  NMR spectrum exhibits seven resonances. This spectral information is thus consistent with a highly symmetric

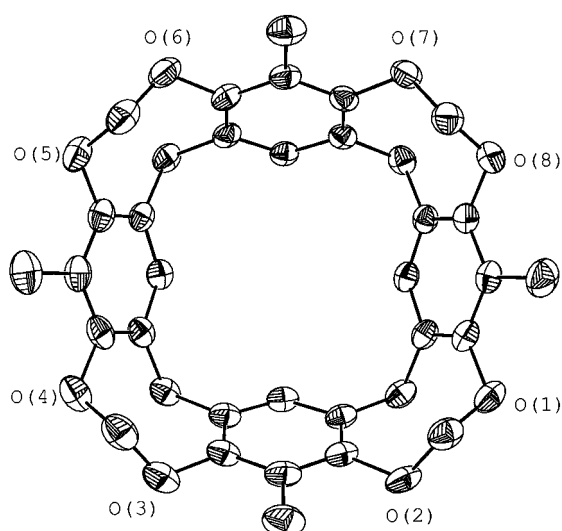


Figure 2. ORTEP plot of the X-ray crystal structure of the [4]cavitand at 30% probability level. Hydrogens are omitted for clarity.

structure, again suggesting a cone conformation ( $C_{5v}$  in this case). This conclusion was further supported by the X-ray diffraction data obtained for single crystals of this compound. The cone conformation obtained from these experiments is shown in Figure 3.

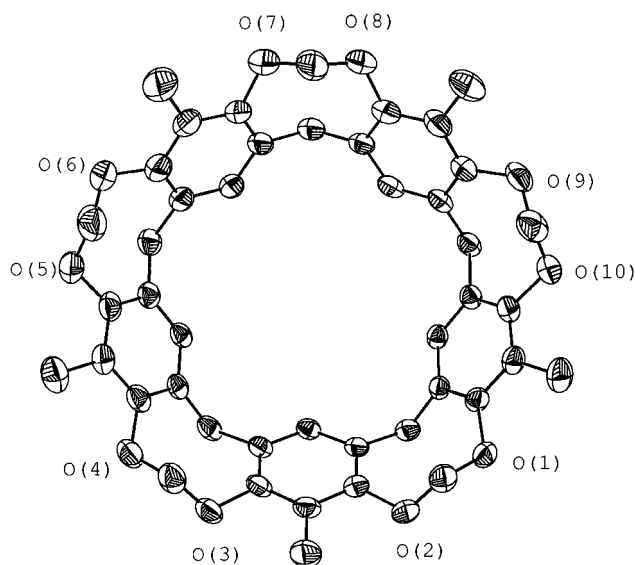


Figure 3. ORTEP plot of the X-ray crystal structure of the [5]cavitand at 30% probability level. Hydrogens are omitted for clarity.

**Characterization of [6]cavitand:** The cone conformation observed for the [4]cavitand and [5]cavitand is not expected to be maintained as more aromatic units are packed in the macrocyclic structure. Steric crowding is anticipated to become so large as to distort the structure, favoring conformations of lower symmetry. Simple molecular mechanics calculations (MM2 force field) suggest that the cone conformation is no longer the most stable one for the [6]cavitand and the [7]cavitand (see Figure 4). The crystal structure of the [6]cavitand (see Figure 6) is almost identical to the “rectan-

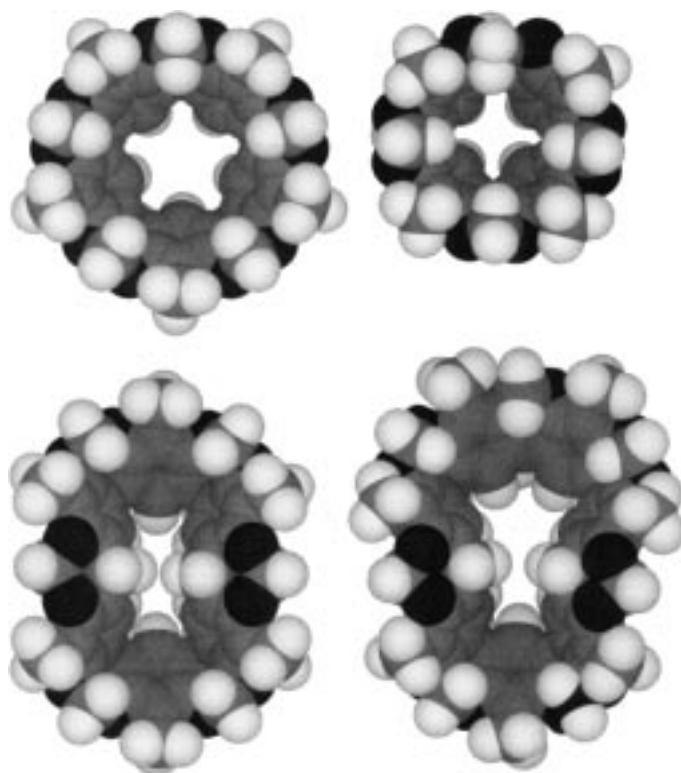


Figure 4. Energy minimized structures of [n]cavitands as obtained using the MM2 force field. [4]Cavitand (top right), [5]cavitand (top left), [6]cavitand], (bottom left) and [7]cavitand (bottom right).

gular”  $C_{2v}$  conformation predicted by molecular mechanics calculations. This structure is also apparent in solution, as supported by the  $^1\text{H}$  NMR spectra of the [6]cavitand. At  $-8^\circ\text{C}$  at 400 MHz in  $\text{CDCl}_3$ , there are four doublets each of major and minor intensities corresponding to the bridge ( $\text{OCH}_2\text{O}$  and  $\text{ArCH}_2\text{Ar}$ ) protons ( $\text{H}_3\text{--H}_{10}$ , Figure 1; see Figure 5 for assignments).<sup>[15]</sup> In addition, there are two singlets each (intensity ratio 2:1) for the aromatic protons ( $\text{H}_1$  and  $\text{H}_2$ ) and for the methyl protons.

At  $-28^\circ\text{C}$ , long range (four bond) COSY correlations connect the “minor” aromatic protons ( $\text{H}_1$ ) to  $\text{H}_5$  and  $\text{H}_9$  only of the “major” set of the  $\text{ArCH}_2\text{Ar}$  bridge protons (see Figure 5a), whereas the “major” aromatic protons ( $\text{H}_2$ ) have cross peaks to all four different resonances for the  $\text{ArCH}_2\text{Ar}$  protons ( $\text{H}_5$ ,  $\text{H}_8$ ,  $\text{H}_9$ ,  $\text{H}_{10}$ ). These results demonstrate that [6]cavitand exists as a singular entity with  $C_{2v}$  symmetry.

As the temperature is raised from  $-8^\circ\text{C}$  several changes occur in the  $^1\text{H}$  NMR spectra of the [6]cavitand. First, a broadening of all resonances is obvious. Second, peaks corresponding to sets of exchanging protons shift closer to one another until they eventually coalesce. For instance, in  $[\text{D}_7]\text{DMF}$  the two aromatic signals are clear singlets at  $-40^\circ\text{C}$  ( $\text{H}_1$  and  $\text{H}_2$ ), but can no longer be differentiated at  $52^\circ\text{C}$  (data not shown). The bridge ( $\text{OCH}_2\text{O}$  and  $\text{ArCH}_2\text{Ar}$ ) protons show similar behavior, but it was not possible to observe complete coalescence for these hydrogens, even at temperatures as high as  $100^\circ\text{C}$ . However, in  $[\text{D}_6]\text{DMSO}$  coalescence was complete and the spectrum was sharp at  $147^\circ\text{C}$  (Figure 7). These findings suggest a fluxional character of the [6]cavitand host, with equivalent “rectangular”  $C_{2v}$  conformations aver-

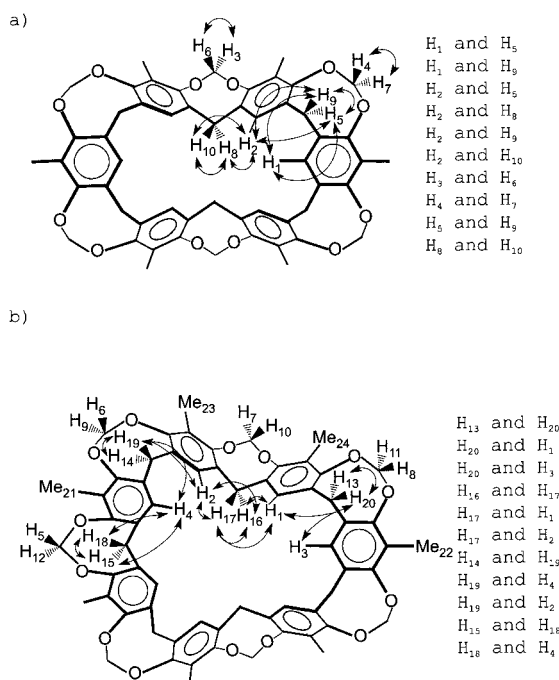


Figure 5. a) Summary of COSY correlations for the [6]cavitand, both short and long range correlations are shown. b) Selected summary of COSY correlations for the [7]cavitand.

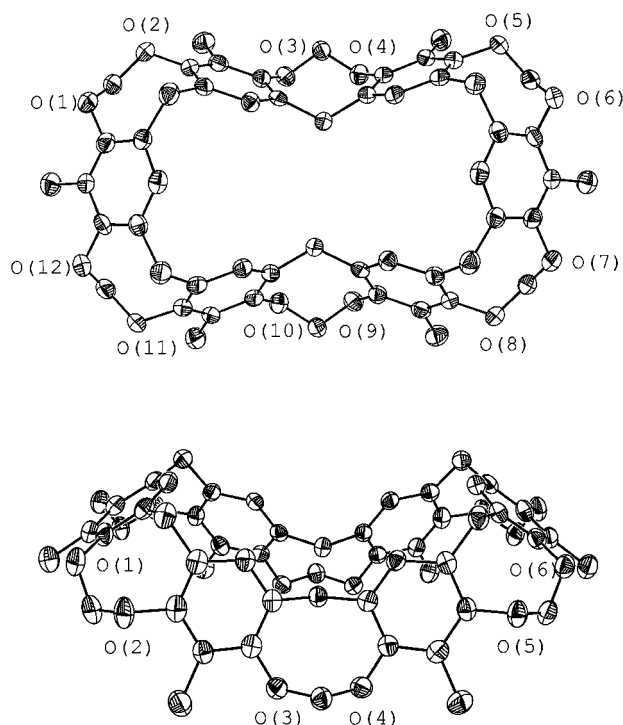
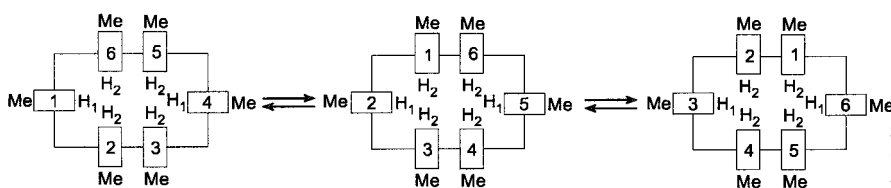


Figure 6. Two views (ORTEP plots at 30% probability levels) of the X-ray crystal structure of the [6]cavitand. Hydrogens are omitted for clarity.



Scheme 1. Interconversion of "minor" ( $H_1$ ) and "major" ( $H_2$ ) proton sets in the [6]cavitand. The numbers 1 to 6 represent the six arenes.

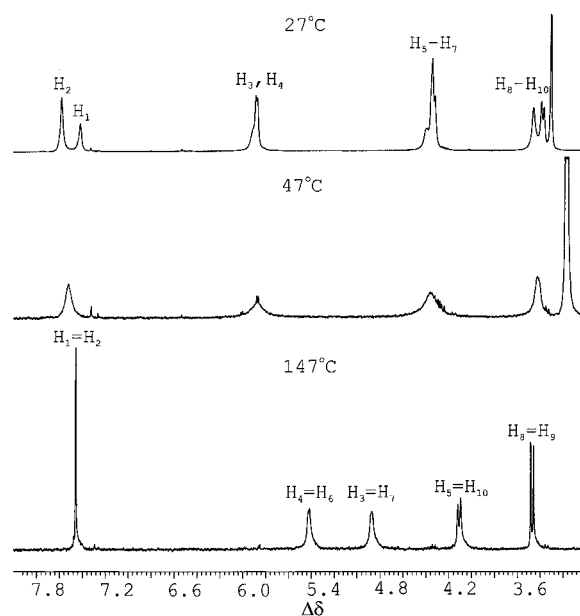


Figure 7. Parts of  $^1\text{H}$  NMR spectra of the [6]cavitand at various temperatures: coalescence of the bridge protons recorded at 500 MHz in  $[\text{D}_6]\text{DMSO}$ .

aging through rapid interconversion at the  $^1\text{H}$  NMR time scale at higher temperature (see Scheme 1). At  $-8^\circ\text{C}$  at 400 MHz in  $\text{CDCl}_3$ , the interconversion process can still be observed in one- and two-dimensional NOESY (EXSY) correlation studies. For instance, irradiation of the "minor"  $H_8$  protons gave a strong negative response (indicating exchange) at the "major"  $H_9$  protons and a positive enhancement (NOE) of the "major"  $H_5$  protons and the "minor"  $H_{10}$  protons (Figure 8a). Likewise, irradiation at  $H_9$  results in a negative response at  $H_8$ ; clearly these two resonances exchange with each other. The positive NOE for  $H_5$  when  $H_8$  was irradiated is due to NOE transfer (NOE build-up at geminal proton  $H_{10}$  followed by NOE transfer via exchange to  $H_5$ ). Similar results were obtained when the other two diarylmethylene bridge protons,  $H_5$  and  $H_{10}$ , were irradiated (see Figure 8b for a summary).<sup>[16]</sup> One-dimensional EXSY spectra<sup>[17]</sup> were recorded in  $\text{CDCl}_3$  at  $-8^\circ\text{C}$  as a function of mixing time ( $t_m$ ) in order to determine the rate for the exchange process. Mixing times of 5 ms and 0.2, 0.4, 0.6 s were employed, and a relaxation delay of 4.0 s was used. The method of analyzing the EXSY spectra is described in the Supporting Information.<sup>[18]</sup> The most reliable determination of the rate constant should be derived from the irradiation of  $H_8$  and  $H_9$ ; the other pairs of exchanging protons suffer from inaccuracies caused by nearby resonances, for instance irradiation of  $H_5$  also irradiated  $H_6$ . The pseudo-first-order rate constant  $k_{\text{obs},8,9}$  was found as  $2.4 \pm 0.1 \text{ s}^{-1}$  whereas  $k_{\text{obs},9,8}$  was  $1.2 \pm 0.1 \text{ s}^{-1}$ . The rate constants for the conversion of the "major" set protons  $H_5$  and  $H_9$  into the

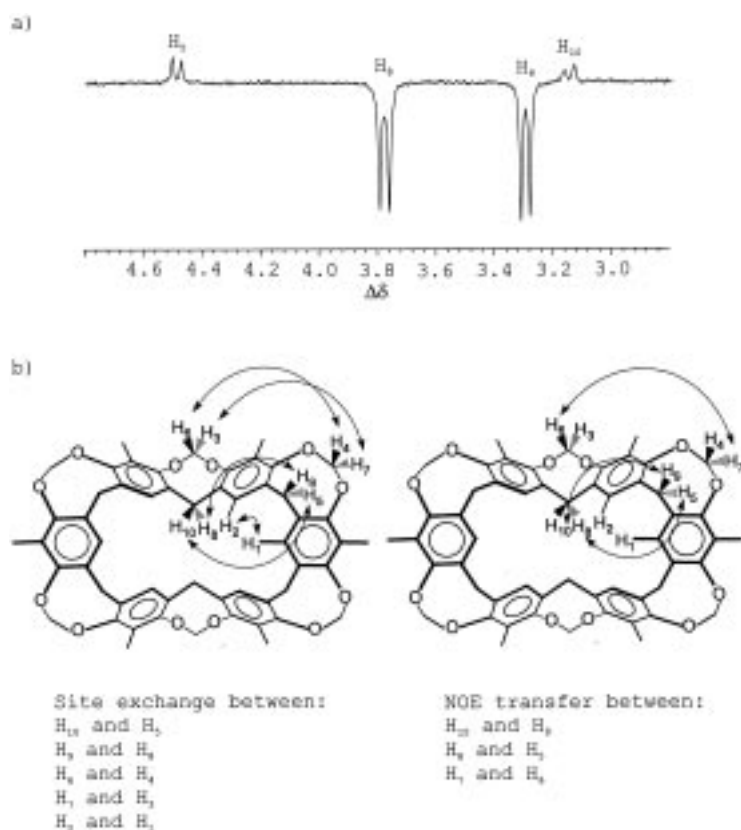


Figure 8. a) 1D NOESY (EXSY) spectrum of the [6]cavitand at 400 MHz in  $\text{CDCl}_3$  at  $-8^\circ\text{C}$ ;  $\text{H}_8$  was irradiated. b) Summary of results of dynamic  $^1\text{H}$  NMR studies on the [6]cavitand at  $27^\circ\text{C}$  to  $-28^\circ\text{C}$ .

“minor” set protons  $\text{H}_{10}$  and  $\text{H}_8$  are half the size of the rate constants for the reverse exchange as required by mass balance.

Green et al. introduced the concept of  $k_{\text{chem}}$ , a modified rate constant, which is “independent of the site population and of the direction in which the rate constant is measured”.<sup>[19]</sup> The general equation for relating  $k_{\text{obs}}$  to  $k_{\text{chem}}$  for an exchange from site A with a population  $p_A$  to site B with a population  $p_B$  was given by Green et al.<sup>[19]</sup> as:

$$k_{\text{chem}} = \frac{p_A + p_B}{p_A p_B} [k_{\text{obs}} (\text{A} \rightarrow \text{B})] N_A \quad (1)$$

where  $N_A$  is the number of nuclei in site from the magnetization is transferred.

Irradiation of a resonance from the minor set (e.g.  $\text{H}_1$ ) leads to magnetization transfer (to  $\text{H}_2$ ) two-thirds of the time. (Scheme 1) Therefore the chemical rate of exchange from  $\text{H}_1$  to  $\text{H}_2$  is 1.5 times the rate of magnetization transfer measured by the NMR experiments ( $k_{\text{obs},1,2}$ ). Irradiation of  $\text{H}_2$  also leads to magnetization transfer two-thirds of the time. Since there are twice as many  $\text{H}_2$  as  $\text{H}_1$  protons,  $N_A$  equals 2; therefore, the chemical rate of exchange from  $\text{H}_2$  to  $\text{H}_1$  is three times of  $k_{\text{obs},2,1}$ . We calculated a  $k_{\text{chem}}$  for the site exchange between  $\text{H}_8$  and  $\text{H}_9$  at  $-8^\circ\text{C}$  in  $\text{CDCl}_3$  as  $3.6 \pm 0.1 \text{ s}^{-1}$ .<sup>[20]</sup>  $\Delta G^\ddagger$  is then given by the expression:<sup>[19]</sup>

$$\Delta G^\ddagger = -RT \ln [k_{\text{chem}} h / k_B T] \quad (2)$$

where  $k_B$  is the Boltzmann constant,  $h$  is Planck's constant,  $R$  is the gas constant, and  $T$  is the temperature. Thus, the free energy of activation for the exchange process,  $\Delta G^\ddagger_{265}$ , is calculated to be  $14.8 \text{ kcal mol}^{-1}$ .

Chemical exchange rate constants can also be determined from the coalescence temperature ( $T_c$ ) of resonances of unequal intensities by solving Equation (3) as described by Shanan-Atidi et al.<sup>[21]</sup> The chemical rate constant is the reciprocal of the average time between jumps,  $\tau$ .<sup>[19, 21, 22]</sup>

$$p_A - p_B = \left( \frac{X^2 - 2}{3} \right)^{3/2} \frac{1}{x} \quad (3)$$

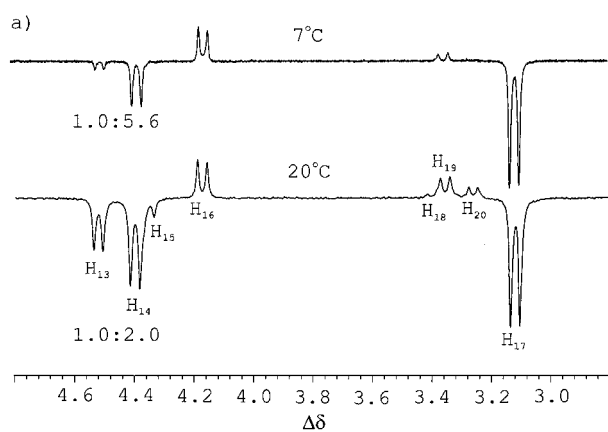
where  $p_A - p_B$  is the population difference of exchanging spins A and B and  $X = 2\pi\Delta\nu\tau$ .

From the  $\Delta\nu$  Equation (3) gives  $\tau$ , and thus  $k_{\text{chem}}$ . Using Equation (2) and putting in  $k_{\text{chem}}$  and the coalescence temperature of the aromatic hydrogens  $\text{H}_1$  and  $\text{H}_2$ , we calculated<sup>[19, 21, 22]</sup> a value of  $15.7 \text{ kcal mol}^{-1}$  for the value of  $\Delta G^\ddagger_{325}$  for the interconversion process in  $[\text{D}_7]\text{DMF}$  (at  $52^\circ\text{C}$ ,  $\Delta\nu = 112.7 \text{ Hz}$  measured at 400 MHz,  $k_{\text{chem}} = 194.3 \text{ s}^{-1}$ <sup>[22]</sup>).

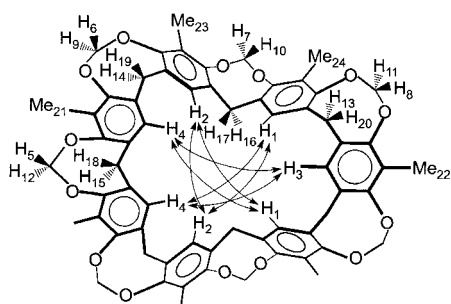
Not surprisingly, the exchange and NOE transfer processes are temperature dependent; at  $-28^\circ\text{C}$  both processes are almost frozen out on the  $^1\text{H}$  NMR time scale, whereas at  $-8^\circ\text{C}$  they are clearly apparent, and at  $2^\circ\text{C}$ , they are more pronounced still. ROESY experiments at  $27^\circ\text{C}$  showed that the negative cross-peaks were due to exchange and not due to dipolar relaxation. Results in  $[\text{D}_7]\text{DMF}$  fully agree with those obtained in  $\text{CDCl}_3$ . Interestingly, at  $-40^\circ\text{C}$  in both  $\text{CDCl}_3$  and  $[\text{D}_7]\text{DMF}$ , all NOE effects observed are negative and their absolute value increases when the temperature is lowered.

**Characterization of [7]cavitand:** The  $^1\text{H}$  NMR spectrum of the [7]cavitand at  $-8^\circ\text{C}$  shows a more complicated pattern than that of the [6]cavitand (Figure 1, see also Figure 1 in the Supporting Information for a full  $^1\text{H}$  NMR spectrum). For instance, four different peaks can be observed for the methyl protons with relative intensities 6:6:6:3. The aromatic hydrogens also show four signals with relative intensities 2:2:2:1. These signals as well as those for the bridge protons (both  $\text{OCH}_2\text{O}$  and  $\text{ArCH}_2\text{Ar}$ ) are fully consistent with a “pinched conformation”, with two well-defined cavities, one slightly larger than the other. This conformation is also in agreement with predictions from molecular mechanics calculations (see Figure 4 and Figure 9). In analogy to the behavior observed with the [6]cavitand (but shifted by at least  $25^\circ\text{C}$  up in temperature), an increase in temperature leads to similar effects on the  $^1\text{H}$  NMR spectrum of the [7]cavitand. Namely, the signals become increasingly broad and tend to coalesce with those peaks corresponding to protons in the same molecular regions. For instance, at  $30^\circ\text{C}$ , the four aromatic signals have merged into three, and at  $60^\circ\text{C}$  only two broad signals can be observed. These spectral features are explained, as in the case of the [6]cavitand, by the interconversion of several equivalent “pinched” conformations.

At  $7^\circ\text{C}$  in  $\text{CDCl}_3$ , long range COSY correlations connect the four aromatic protons ( $\text{H}_1$  to  $\text{H}_4$ ) to the  $\text{ArCH}_2\text{Ar}$  protons. For instance, the  $\text{H}_1$  protons have cross peaks to  $\text{H}_{16}$ ,  $\text{H}_{20}$ , and  $\text{H}_{17}$ , whereas the  $\text{H}_3$  protons only correlate to  $\text{H}_{20}$  (see Figure 5b). ROESY experiments at  $-8^\circ\text{C}$  confirm these



b)



Site exchange between:

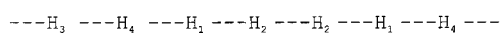
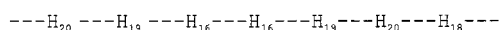
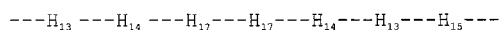


Figure 9. Conformation of the [7]cavitand: a) 1D NOESY (EXSY) spectrum of the [7]cavitand at 400 MHz in  $\text{CDCl}_3$  at 7 °C and 20 °C;  $\text{H}_{17}$  was irradiated. b) Summary of results of dynamic  $^1\text{H}$  NMR studies on the [7]cavitand – 8 °C to 22 °C.

correlations by showing strong NOE cross peaks between the aromatic protons ( $\text{H}_1$  to  $\text{H}_4$ ) and the four more upfield  $\text{ArCH}_2\text{Ar}$  resonances ( $\text{H}_{17}$  to  $\text{H}_{20}$ ).<sup>[23]</sup> Again, the  $\text{H}_3$  protons connect to  $\text{H}_{20}$ , and  $\text{H}_1$  connects with  $\text{H}_{17}$  and  $\text{H}_{20}$ . Also, there are weak negative cross peaks (indicating exchange) between  $\text{H}_{16}$  and  $\text{H}_{19}$ , and  $\text{H}_{14}$  and  $\text{H}_{17}$ . One-dimensional EXSY spectra were recorded at different temperatures varying mixing times to study the interconversion process between the different  $\text{ArCH}_2\text{Ar}$  resonances. At 7 °C (at 400 MHz in  $\text{CHCl}_3$ ) at short mixing times (50 ms), irradiation of  $\text{H}_{17}$  results in a negative response (indicating exchange) at  $\text{H}_{14}$  only. At longer mixing times (100 to 400 ms), irradiation results in negative responses at  $\text{H}_{13}$  and  $\text{H}_{14}$ . However, the ratio between the intensities for those two resonances changes with mixing times, from 1:44 at 100 ms to 1:5.6 at 400 ms. Also, at the latter mixing time, a small negative response at  $\text{H}_{15}$  is found. At higher temperature (20 °C), irradiation of  $\text{H}_{17}$  yields an even more pronounced response at  $\text{H}_{13}$  and at  $\text{H}_{15}$  (intensity ratio between  $\text{H}_{13}:(\text{H}_{14}/\text{H}_{15}) = 1:2.0$  at 400 ms mixing time, see Figure 9a),<sup>[24]</sup> and the major response ( $\text{H}_{14}$ ) decreases with increasing mixing time relative to the secondary responses ( $\text{H}_{13}$  and  $\text{H}_{15}$ ). Irradiation of  $\text{H}_{13}$  at 7 °C yields equal negative responses at

$\text{H}_{14}$  and  $\text{H}_{15}$ . The ratio between  $\text{H}_{14}$  and  $\text{H}_{15}$  does not change with mixing times, but at longer mixing times (250 to 400 ms) a small negative response at  $\text{H}_{17}$  appears. The ratio between the combined intensities for  $\text{H}_{14}$  and  $\text{H}_{15}$  to the one for  $\text{H}_{17}$  changes from 22:1 at 250 ms to 13.2:1 at 400 ms.<sup>[25]</sup> Similar results are found for the other exchanging protons, and for the second exchange set of the  $\text{ArCH}_2\text{Ar}$  protons ( $\text{H}_{16}$ ,  $\text{H}_{18}$  to  $\text{H}_{20}$ ). Figure 9b summarizes the above results. It seems that the two unequal cavities in [7]cavitand exchange with each other. Scheme 2 explains the interconversion process and is consistent with the observed NMR data. The two resonances  $\text{H}_{13}$  and  $\text{H}_{17}$  exchange only weakly in comparison to  $\text{H}_{14}$  and  $\text{H}_{17}$  because both are correlated by a two step exchange process. In the first step, one  $\text{H}_{17}$  proton exchanges with  $\text{H}_{14}$ , which exchanges with  $\text{H}_{13}$  in a second step. The more  $\text{H}_{14}$  is produced during irradiation of  $\text{H}_{17}$  (by a higher temperature or longer mixing time), the more  $\text{H}_{13}$  can be observed to respond.

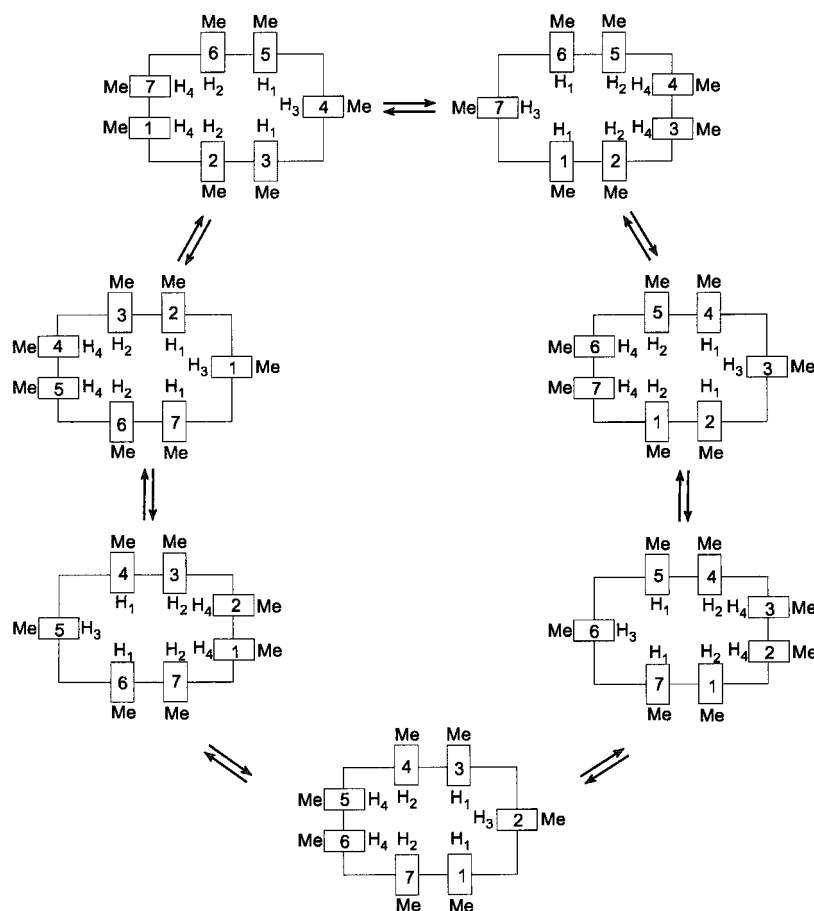
At 7 °C the pseudo-first-order rate constant  $k_{\text{obs},14,17}$  was found as  $1.4 \pm 0.1 \text{ s}^{-1}$  whereas  $k_{\text{obs},17,14}$  was  $0.7 \pm 0.1 \text{ s}^{-1}$ . The rate constants for the conversion of the  $\text{H}_{17}$  protons into the  $\text{H}_{14}$  protons are half the size of the rate constants for the reverse exchange as required by mass balance since only one  $\text{H}_{14}$  proton exchanges with  $\text{H}_{17}$ . The other  $\text{H}_{14}$  proton exchanges with  $\text{H}_{13}$  and the second  $\text{H}_{17}$  stays  $\text{H}_{17}$  at any given step. When  $\text{H}_{14}$  is irradiated, magnetization transfer to both  $\text{H}_{13}$  and  $\text{H}_{17}$  is observed. Magnetization transfer from  $\text{H}_{14}$  to either site occurs on average one third of the time. The chemical rate of exchange from  $\text{H}_{14}$  to  $\text{H}_{17}$  is three times the rate of magnetization transfer measured by the NMR experiments ( $k_{\text{obs},14,17}$ ). In contrast,  $k_{\text{chem}}$  for the interconversion of  $\text{H}_{17}$  to  $\text{H}_{14}$  is six times  $k_{\text{obs},17,14}$ , since a  $\text{H}_{17}$  proton is a bystander and does not participate in any given exchange step. We calculated a  $k_{\text{chem}}$  for the site exchange between  $\text{H}_{17}$  and  $\text{H}_{14}$  at 7 °C in  $\text{CDCl}_3$  as  $4.2 \pm 0.1 \text{ s}^{-1}$ .<sup>[20]</sup>  $\Delta G_{280}^\ddagger$  is calculated to be  $15.6 \text{ kcal mol}^{-1}$ .

The  $k_{\text{chem}}$  for the [6]cavitand is somewhat higher than that for the [7]cavitand at the same temperature ( $k_{\text{obs},8,9} = 11.1 \pm 0.1 \text{ s}^{-1}$ ,  $k_{\text{obs},9,8} = 5.5 \pm 0.1 \text{ s}^{-1}$ ,  $k_{\text{chem}} = 16.5 \pm 0.1 \text{ s}^{-1}$ ).

As in the case of the [6]cavitand, at low temperature all NOEs turned out to be negative and their absolute values were small at –15 °C. Lowering the temperature to –40 °C yielded stronger NOE signals. These experiments allowed complete assignment of all the hydrogens for the [7]cavitand. For instance, irradiation of protons  $\text{H}_7$  resulted in a negative enhancement of the methyl signals  $\text{H}_{23}$  and  $\text{H}_{24}$  (both –4 %) and of the geminal protons  $\text{H}_{10}$  (–56 %), a result consistent with COSY experiments at low temperature. Similarly, irradiation of the methyl signal  $\text{Me}_{24}$  produced a decrease on signals  $\text{H}_7$ ,  $\text{H}_8$ ,  $\text{H}_{10}$  and  $\text{H}_{11}$  (Figure 9). Following this methodology, complete assignment of all protons for the [7]cavitand was made (see Supporting Information for a complete list of all NOE relationships and assignment of all protons).

## Conclusions

We have developed a simple procedure to synthesize the first cavitands containing more than four aromatic units. Addi-



Scheme 2. Interconversion of proton sets in the [7]cavitand. The numbers 1 to 7 represent the seven arenes.

tionally, these are the first cavitands reported with no “feet”. The low-order [*n*]cavitands (*n* = 4, 5) adopt a rigid cone-like conformation, identical to that previously reported by Cram and co-workers, with no degree of conformational mobility. On the other hand, the higher-order [*n*]cavitands (*n* = 6, 7) manifest lower symmetry, and show some flexibility at room temperature, with interconversion between equivalent conformations. These structures exhibit two cavities, rather than one. The cavities are identical for the [6]cavitand, while one is slightly larger than the other for the [7]cavitand. The departure from the typical cone-like conformation for these two larger cavitands is presumably due to steric crowding. These “pinched” conformations are clearly observed by <sup>1</sup>H NMR spectroscopy at lower temperatures, at which the conformational interconversion processes are sufficiently slow.

An important feature common to all these new cavitands is the presence of benzylic methyl groups in the upper rim of the molecule. Efforts aimed at the functionalization of such positions are currently underway in our research groups. We anticipate that this work may lead to the design and synthesis of new and interesting hosts, opening the way to a new generation of enlarged cavitands and their derivatives, such as hemicarcerands and hemicarceplexes. Preliminary results are already in hand for the first hemicarceplex with a C<sub>5</sub> axis of symmetry. The host properties of these novel compounds may offer many exciting possibilities.

## Experimental Section

**Synthesis of resorcin[4]arene (Octol) and [4]cavitand:** In a flask provided with stirring and a condenser a mixture of 2-methylresorcinol (3.00 g, 24.2 mmol), formaldehyde solution (20 mL, 35% aqueous solution), EtOH (40 mL) and concentrated hydrochloric acid (15 mL) was kept at 80 °C. After 48 h the reaction mixture was cooled down and filtered. The precipitate was washed with abundant water (400 mL). The product was dried at 80 °C in vacuo for 24 h to yield octol (2.41 g, 73.1%).

A mixture of octol (0.90 g, 1.65 mmol), Cs<sub>2</sub>CO<sub>3</sub> (3.00 g), CH<sub>2</sub>BrCl (6.5 mL) and DMF (15 mL) was stirred for 8 h in a sealed tube at 92 °C. After cooling, the reaction content was poured in a hot (around 60–80 °C) mixture (CAUTION!) of HCl (15 mL) and H<sub>2</sub>O (250 mL) and stirred for a while until the remaining CH<sub>2</sub>BrCl fully evaporated. After cooling, the mixture was filtered and washed with abundant water. This crude was purified by chromatography with CHCl<sub>3</sub>/hexanes, and after drying under vacuum yielded [4]cavitand (0.815 g, 1.38 mmol, 83%). <sup>1</sup>H NMR (500 MHz, CDCl<sub>3</sub>, 27 °C): δ = 6.98 (s, 4H; ArH), 5.87 (d, <sup>2</sup>J(H,H) = 6.9 Hz, 4H; OCH<sub>2</sub>O), 4.44 (d, <sup>2</sup>J(H,H) = 12.2 Hz, 4H; ArCH<sub>2</sub>-Ar), 4.30 (d, <sup>2</sup>J(H,H) = 6.9 Hz, 4H; OCH<sub>2</sub>O), 3.23 (d, <sup>3</sup>J(H,H) = 12.2 Hz, 4H; ArCH<sub>2</sub>Ar), 1.96 (s, 12H; ArCH<sub>3</sub>); <sup>13</sup>C NMR (100 MHz, CDCl<sub>3</sub>, 27 °C): δ = 153.6, 135.2, 125.2, 124.3, 99.0, 34.0, 10.2; HRMS (+LSIMS, thioglycerol): 593.21767. Dev: 0.21 ppm.

**Synthesis of higher resorcin[*n*]arenes and [*n*]cavitands:** A mixture of 2-methyl resorcinol (20.0 g, 161.1 mmol), diethoxymethane (20 mL, 161.1 mmol), and EtOH (360 mL) was heated to 60 °C. After 15 min concentrated HCl (90 mL) was added, and the mixture was stirred at 60 °C for 30 min. The reaction content was then poured into a 2 L flask that contained water (750 mL) and ethyl acetate (250 mL). After separation of the two phases, the aqueous phase was extracted twice with ethyl acetate (100 mL). The combined organic phases were washed with water until the aqueous phase proved neutral. Ethyl acetate was removed under reduced pressure, and the resulting solid was dried at 80 °C under vacuum for one hour to yield the resorcinarene mixture (24 g). The crude product was dissolved in DMA (360 mL). K<sub>2</sub>CO<sub>3</sub> (50 g, 362 mmol) was added, and the mixture was heated to 60 °C under a nitrogen atmosphere. Bromochloromethane (24 mL, 369.6 mmol) was added after 30 min, and the reaction was stirred overnight at 60 °C. After cooling, the reaction mixture was filtered through Celite which was washed with abundant chloroform. The solvent was then removed under reduced pressure to yield a brown solid that was dissolved in chloroform (100 mL) and subjected to column chromatography (600 g silica gel, 230–400 mesh). Using chloroform as the eluent an yellowish solid was obtained (5.2 g). Ethyl acetate (100 mL) was added to this solid. The mixture was sonicated for 5 min and filtered. The white precipitate (mixture of [5]cavitand and [6]cavitand only) was dissolved in chloroform (100 mL), and the mixture was shortly heated (heatgun), sonicated for 5 min and filtered, yielding the first batch of [6]cavitand (0.80 g). The filtrate was reduced in volume to about 50 mL volume and refrigerated overnight, resulting in the precipitation of more [6]cavitand (2.1 g). The subsequent filtrate was reduced to about 15 mL of chloroform, and ethyl acetate (50 mL) was added. After the reaction mixture was refrigerating for 30 min, the precipitate was removed by filtration to yield most of the [5]cavitand as a white solid (0.86 g, 3.6%). At this point, the two filtrates were combined, and the solvent was evaporated to yield a

yellowish solid that contained mainly [4]cavitand and [7]cavitand in addition to some [6]cavitand and more polar and coloured products. The solid was purified by column chromatography using chloroform as the mobile phase. The less polar fractions were combined, the solvent was removed, and the solid was put in ethyl acetate (50 mL) and filtered to yield [6]cavitand (0.3 g). The filtrate was reduced in volume and refrigerated overnight to yield [4]cavitand as colorless needles (0.87 g, 3.6%).

The more polar fractions containing [7]cavitand were combined, the solvent was evaporated, and ethyl acetate (25 mL) was added. The precipitate (0.1 g) gave additional [6]cavitand (3.3 g total, 13.9% for two steps). The filtrate was treated with hexanes to yield [7]cavitand as a white powder (0.28 g, 1.1%).

**[5]Cavitand:**  $^1\text{H}$  NMR (500 MHz,  $\text{CDCl}_3$ , 27 °C):  $\delta$  = 7.16 (s, 5H; ArH), 5.97 (d,  $^2J(\text{H,H})$  = 7.0 Hz, 5H;  $\text{OCH}_2\text{O}$ ), 4.35 (d,  $^2J(\text{H,H})$  = 13.0 Hz, 5H;  $\text{ArCH}_2\text{Ar}$ ), 4.33 (d,  $^2J(\text{H,H})$  = 7.0 Hz, 5H;  $\text{OCH}_2\text{O}$ ), 3.37 (d,  $^2J(\text{H,H})$  = 13.0 Hz, 5H;  $\text{ArCH}_2\text{Ar}$ ), 2.04 (s, 15H;  $\text{ArCH}_3$ );  $^{13}\text{C}$  NMR (100 MHz,  $\text{CDCl}_3$ , 27 °C):  $\delta$  = 155.4, 132.3, 128.1, 124.4, 100.1, 35.3, 10.3; HRMS (+LSIMS, thioglycerol): 741.26992; Dev: -0.07 ppm.

**[6]Cavitand:**  $^1\text{H}$  NMR (500 MHz,  $\text{CDCl}_3$ , -13 °C):  $\delta$  = 7.19 (s, 2H; ArH), 7.14 (s, 4H; ArH), 5.92 (d,  $^2J(\text{H,H})$  = 7.3 Hz, 2H;  $\text{OCH}_2\text{O}$ ), 5.88 (d,  $^2J(\text{H,H})$  = 6.7 Hz, 4H;  $\text{OCH}_2\text{O}$ ), 4.49 (d,  $^2J(\text{H,H})$  = 11.9 Hz, 4H;  $\text{ArCH}_2\text{Ar}$ ), 4.43 (d,  $^2J(\text{H,H})$  = 6.9 Hz, 2H;  $\text{OCH}_2\text{O}$ ), 4.28 (d,  $^2J(\text{H,H})$  = 7.0 Hz, 4H;  $\text{OCH}_2\text{O}$ ), 3.78 (d,  $^2J(\text{H,H})$  = 13.1 Hz, 2H;  $\text{ArCH}_2\text{Ar}$ ), 3.30 (d,  $^2J(\text{H,H})$  = 11.7 Hz, 4H;  $\text{ArCH}_2\text{Ar}$ ), 3.16 (d,  $^2J(\text{H,H})$  = 12.8 Hz, 2H;  $\text{ArCH}_2\text{Ar}$ ), 2.01 (s, 12H;  $\text{ArCH}_3$ ), 1.97 (s, 6H;  $\text{ArCH}_3$ );  $^{13}\text{C}$  NMR (100 MHz,  $\text{CDCl}_3$ , 27 °C):  $\delta$  = 156.1, 154.2, 153.3, 135.4, 134.3, 130.8, 127.7, 125.0, 124.5, 123.9, 102.0, 99.1, 37.4, 33.5, 9.9; HRMS (LSIMS, thioglycerol): 889.32214; Dev: -0.30 ppm.

**[7]Cavitand:**  $^1\text{H}$  NMR (400 MHz,  $[\text{D}_7]\text{DMF}$ , -15 °C):  $\delta$  = 7.64 (s, 2H; ArH), 7.52 (s, 2H; ArH), 7.34 (s, 1H; ArH), 7.32 (s, 2H; ArH), 6.10–6.08 (m, 3H;  $\text{OCH}_2\text{O}$ ), 6.00 (d,  $^2J(\text{H,H})$  = 7.3 Hz, 2H;  $\text{OCH}_2\text{O}$ ), 5.94 (d,  $^2J(\text{H,H})$  = 7.7 Hz, 2H;  $\text{OCH}_2\text{O}$ ), 4.56–4.51 (m, 4H;  $\text{OCH}_2\text{O}$ ), 4.46–4.42 (m, 5H;  $\text{OCH}_2\text{O}$ ,  $\text{ArCH}_2\text{Ar}$ ), 4.33 (d,  $^2J(\text{H,H})$  = 12.1 Hz, 2H;  $\text{ArCH}_2\text{Ar}$ ), 4.23 (d,  $^2J(\text{H,H})$  = 12.8 Hz, 1H;  $\text{ArCH}_2\text{Ar}$ ), 3.76 (d,  $^2J(\text{H,H})$  = 11.7 Hz, 2H;  $\text{ArCH}_2\text{Ar}$ ), 3.56–3.50 (m, 3H;  $\text{ArCH}_2\text{Ar}$ ), 3.40 (d,  $^2J(\text{H,H})$  = 11.7 Hz, 2H;  $\text{ArCH}_2\text{Ar}$ ), 2.07 (s, 2H;  $\text{ArCH}_3$ ), 2.05 (s, 1H;  $\text{ArCH}_3$ ), 2.03 (s, 2H;  $\text{ArCH}_3$ ), 1.90 (s, 2H;  $\text{ArCH}_3$ );  $^{13}\text{C}$  NMR (100 MHz,  $[\text{D}_7]\text{DMF}$ , 22 °C):  $\delta$  = 156.0, 155.2, 155.1, 155.0, 154.5, 154.0, 153.4, 135.8, 135.7, 133.8, 133.4, 133.2, 132.5, 127.7, 127.2, 126.8, 125.5, 125.3, 125.1, 125.0, 100.9, 100.4, 100.3, 99.3, 34.6, 33.4, 9.9, 9.8, 9.7; HRMS (LSIMS, thioglycerol): 1036.36642; Dev: -0.57 ppm.

**X-ray Crystallography:** Single crystals of all compounds were grown by slow evaporation of their  $\text{CHCl}_3$  solutions. X-ray intensity data for crystals of [4]cavitand (**4**) and [6]cavitand (**6**) were measured at 27 °C on a Bruker SMART 1000 CCD-based X-ray diffractometer system equipped with a Mo-target X-ray tube ( $\lambda$  = 0.71073 Å). For the X-ray crystallographic analysis of **6** we used a colorless plate of approximate dimensions  $0.22 \times 0.18 \times 0.07 \text{ mm}^3$ , which was wedged into a quartz capillary filled with a mixture of mineral oil and chloroform (1:1 v/v). For the X-ray crystallographic analysis of **4** we used a clear parallel block of approximate dimensions  $0.44 \times 0.25 \times 0.22 \text{ mm}^3$  cemented onto a quartz fiber with epoxy glue. Data were measured using omega scans of  $0.3^\circ$  per frame for 10 seconds such that a hemisphere was collected. A total of 1271 frames were collected with a final resolution of 0.75 Å. Significant decays (18% in **6** and 5% in **4**) were indicated by the recollection of the first 50 frames at the end of data collection. The frames were integrated with the Bruker SAINT software package using a narrow-frame integration algorithm, which also corrects for decay, Lorentz, and polarization effects.<sup>[26]</sup> Absorption corrections were applied using SADABS supplied by George Sheldrick.<sup>[27]</sup>

The structures of **4** and **6** were solved and refined using the Bruker SHELXTL (Version 5.1) Software Package<sup>[28–30]</sup> in the space groups  $C2/c$  and  $Pbca$ , respectively. Direct methods revealed that the asymmetric unit of **6** consists of one half of the molecule that is related to the other half by a crystallographic two-fold axis. Further refinement revealed the presence of three chloroform molecules in the asymmetric unit, two of which are disordered and refined with the C–Cl bond distance restraints. The asymmetric unit of **4** contains two independent cavitand molecules and three lattice  $\text{CHCl}_3$ . The latter are all disordered and were refined with

C–Cl bond distance restraints. With all non-hydrogen atoms being anisotropic and all hydrogen atoms in calculated position and riding mode, the structure was refined to convergence by least squares method on  $F^2$ , SHELXL-93, as incorporated in SHELXTL.PC V 5.03. The final least-squares refinements converged at the R-factors reported in Table 1, along with other procedural parameters.

Table 1. Crystallographic data.

	[4]Cavitand	[5]Cavitand	[6]Cavitand
formula	$\text{C}_{75}\text{H}_{65}\text{O}_{16}\text{Cl}_9$	$\text{C}_{50}\text{H}_{49}\text{O}_{11}\text{Cl}_9$	$\text{C}_{30}\text{H}_{27}\text{O}_6\text{Cl}_9$
<i>FW</i>	1541.32	1145.01	802.57
space group	<i>Pbca</i>	$C2/c$	$C2/c$
<i>a</i> [Å]	18.0491(15)	38.955(4)	29.696(9)
<i>b</i> [Å]	20.5461(17)	12.485(1)	10.306(3)
<i>c</i> [Å]	38.411(3)	26.410(3)	22.988(7)
$\beta$ [°]	90	127.63(1)	93.045(6)
<i>V</i> [Å <sup>3</sup> ]	14244(2)	10172(2)	7026(4)
<i>Z</i>	8	8	8
$\rho_{\text{calcd}}$ [g cm <sup>-3</sup> ]	1.437	1.50	1.518
radiation	$\text{MoK}\alpha$	$\text{MoK}\alpha$	$\text{MoK}\alpha$
$\mu$ [mm <sup>-1</sup> ]	0.423	0.56	0.758
<i>T</i> [°C]	27	-100	27
<i>Rs</i> (all data)	<i>R</i> = 0.1113, <i>wR2</i> = 0.1840	<i>R</i> = 0.192, <i>Rw</i> = 0.277	<i>R</i> = 0.1411, <i>wR2</i> = 0.2072
<i>Rs</i> (observed data)	<i>R</i> = 0.0517, <i>wR2</i> = 0.1348	<i>R</i> = 0.098, <i>Rw</i> = 0.128	<i>R</i> = 0.0745, <i>wR2</i> = 0.1843

$$R = \frac{\sum |F_o| - |F_c|}{\sum |F_o|}, \quad R_w = \frac{(\sum (F_o^2 - F_c^2)^2 / \sum w(F_o^2)^2)^{1/2}}{\sum w(F_o^2)^2}, \quad wR2 = \frac{(\sum w(F_o^2 - F_c^2)^2)^{1/2}}{\sum w(F_o^2)^2}$$

A crystal of [5]cavitand (**5**) was mounted on a glass fiber and data were collected at -100 °C on a Rigaku/ADSC CCD area detector. Two sets of scans were collected ( $\varphi$  = 0.0 to 190.0°,  $\chi$  = -90°; and  $\omega$  = -18.0 to 23.0°,  $\chi$  = -90°, 0.30° oscillations; 58.0 s exposures). The data were processed using the d<sup>8</sup>TREK program<sup>[31]</sup> and corrected for Lorentz and polarization effects. The structure was solved by direct methods<sup>[32]</sup> and expanded using Fourier techniques.<sup>[33]</sup> The crystals of **5** formed with one cavitand molecule along with three molecules of chloroform and one ethanol molecule in the asymmetric unit. The atoms of the solvent molecules were refined isotropically while all atoms comprising the cavitand were refined anisotropically. The material was only weakly diffracting, likely as a result of the large amount of disordered, volatile solvent in the lattice. It is this weak diffraction that gives rise to the relatively large residuals (see Table 1), however there do not appear to be any abnormal geometries or thermal parameters associated with the cavitand moiety. All calculations were performed with the teXsan crystallographic software package from Molecular Structure Corporation.<sup>[34]</sup>

Crystallographic data (excluding structure factors) for the structures reported in this paper have been deposited with the Cambridge Crystallographic Data Centre as supplementary publication no. CCDC-148476 (for **4**), CCDC-148477 (**6**), and CCDC-148662 (**5**). Copies of the data can be obtained free of charge on application to CCDC, 12 Union Road, Cambridge CB2 1EZ, UK (fax: (+44) 1223-336-033; e-mail: deposit@ccdc.cam.ac.uk).

## Acknowledgement

The authors acknowledge the NSF (to AEK, CHE-9633434 and CHE-9982014), NSERC (JCS), and NIH (JCS, GM56104) for the support of this research work. C.P. is grateful to Xunta de Galicia for a postdoctoral fellowship and E.R. thanks the University of Miami for a Maytag graduate fellowship. T.R. acknowledges the CCD diffractometer fund from the University of Miami.



- [1] D. J. Cram, J. M. Cram in *Container Molecules and Their Guests*, Monographs in Supramolecular Chemistry (Ed.: J. F. Stoddart), Royal Society of Chemistry, Cambridge, **1994**, Chapter 5.
- [2] A. G. S. Högberg, *J. Org. Chem.* **1980**, *45*, 4498.
- [3] L. M. Tunstad, J. A. Tucker, E. Dalcanales, J. Weiser, J. A. Bryant, J. C. Sherman, R. C. Helgeson, C. B. Knobler, D. J. Cram, *J. Org. Chem.* **1989**, *54*, 1305.
- [4] J. A. Bryant, C. B. Knobler, D. J. Cram, *J. Am. Chem. Soc.* **1990**, *112*, 1254.
- [5] D. J. Cram, S. Karbach, H.-E. Kim, C. B. Knobler, E. F. Maverick, J. L. Ericson, R. C. Helgeson, *J. Am. Chem. Soc.* **1988**, *110*, 2229.
- [6] For a recent and comprehensive review, see: A. Jasat, J. C. Sherman, *Chem. Rev.* **1999**, *99*, 931.
- [7] D. R. Stewart, C. D. Gutsche, *J. Am. Chem. Soc.* **1999**, *121*, 4136.
- [8] K. A. Connors, *Chem. Soc. Rev.* **1997**, *97*, 1325.
- [9] P. Timmerman, W. Verboom, D. N. Reinhoudt, *Tetrahedron* **1996**, *52*, 2663.
- [10] H. Konishi, K. Ohata, O. Morikawa, K. Kobayashi, *J. Chem. Soc. Chem. Commun.* **1995**, 309.
- [11] H. Konishi, T. Nakamura, K. Ohata, K. Kobayashi, O. Morikawa, *Tetrahedron Lett.* **1996**, *37*, 7383.
- [12] Parts of this work were presented at the 218th ACS National Meeting held in New Orleans, **1999**.
- [13] In analogy with the nomenclature of the  $[n]$ cyclophanes, we have decided to name these hosts as  $[n]$ cavitands, where  $n$  is the number of aromatic subunits in the macrocycle.
- [14] E. Román, C. Peinador, S. Mendoza, A. E. Kaifer, *J. Org. Chem.* **1999**, *64*, 2577.
- [15] Further assignments of the geminal pairs of protons were made after studies of both crystal structure and CPK models in consideration of the shielding environments. Additionally, NOE experiments were used at low temperature. For instance, H<sub>3</sub> sits closer to acetal oxygens than does H<sub>9</sub>, whereas H<sub>9</sub> is closer to the aromatic protons H<sub>1</sub> and H<sub>2</sub>. A stronger NOE between H<sub>9</sub> and H<sub>1</sub> or H<sub>2</sub> is expected; and the stronger NOE is observed with the more shielded proton, which we therefore assign as H<sub>9</sub>.
- [16] Saturation transfer experiments also support the conformational exchange processes in this host. At 300 K in CDCl<sub>3</sub> irradiation of the protons (2H) at  $\delta = 3.79$  led to the disappearance of the protons at  $\delta = 3.35$  (4H), providing additional evidence that they exchange with one another.
- [17] Pulse sequence used: selnpgp. 2 (Bruker, Avance-version (00/02/07): 1D NOESY using selective excitation with a shaped pulse; dipolar coupling may be due to NOE or chemical exchange. Figure 8a shows a typical spectrum.
- [18] To extract the rate constants from the EXSY spectra, the full matrix approach described in: C. L. Perrin, R. K. Gipe, *J. Am. Chem. Soc.* **1984**, *106*, 4036 was used; see also C. L. Perrin, T. J. Dwyer, *Chem. Rev.* **1990**, *90*, 935.
- [19] M. L. H. Green, L.-L. Wong, A. Sella, *Organometallics* **1992**, *11*, 2660.
- [20] A full error analysis has not been attempted. The rate constants are averaged between the different mixing times.
- [21] H. Shanan-Atidi, K. H. Bar-Eli, *J. Phys. Chem.* **1970**, *74*, 961.
- [22] Note that  $k_{\text{chem}} = k_{1,2} + k_{2,1} = 1.5 k_{1,2} = 3 k_{2,1}$  since  $p_1 k_{1,2} = p_2 k_{2,1}$  (mass balance requirement).
- [23] Assignments were made as outlined in ref. [15].
- [24] H<sub>14</sub> and H<sub>15</sub> are not fully resolved, their relative integration cannot be obtained accurately.
- [25] Irradiation of the multiplet that contains H<sub>14</sub> and H<sub>15</sub> (and the upfield ArOCH<sub>2</sub>OAr resonances) yields responses by H<sub>13</sub> and H<sub>17</sub> at a constant 1.5:1 ratio. There are also responses by the downfield ArOCH<sub>2</sub>OAr protons.
- [26] *SAINT V 6.035*, Software for the CCD Detector System, Bruker-AXS, **1999**.
- [27] B. Blessing, *Acta Crystallogr.* **1995**, *A51*, 33.
- [28] G. M. Sheldrick, *SHELXS-90*, Program for the Solution of Crystal Structures, University of Göttingen, Germany, **1990**.
- [29] G. M. Sheldrick, *SHELXL-93*, Program for the Refinement of Crystal Structures, University of Göttingen, Germany, **1993**.
- [30] *SHELXTL 5.03 (WINDOW-NT Version)*, Program Library for Structure Solution and Molecular Graphics, Bruker-AXS, **1998**.
- [31] *d\*TREK*, Area detector software, Version 4.13, Molecular Structure Corporation, **1996–1998**.
- [32] A. Altomare, M. C. Burla, G. Cammali, M. Cascarano, C. Giacovazzo, A. Guagliardi, A. G. G. Moliterni, G. Polidori, A. Spagna, SIR97: A new tool for crystal structure determination and refinement, *J. Appl. Crystallogr.* **1999**, *32*, 115.
- [33] P. T. Beurskens, G. Admiraal, G. Beurskens, W. P. Bosman, R. de Gelder, R. Israel, J. M. M. Smits, The DIRDIF-94 program system, Technical Report of the Crystallography Laboratory, University of Nijmegen, The Netherlands, **1994**.
- [34] *teXan*, Crystal Structure Analysis Package, Molecular Structure Corporation, **1996–1998**.

Received: August 28, 2000 [F2698]